

Experimental Results on the Control of Cooperative Robots without Velocity Measurements

Marco A. Arteaga

Sección de Eléctrica, DEPMI

Universidad Nacional Autónoma de México

Apdo. Postal 70-256, México, D. F., 04510, México,

Tel.: + 52 55-56-22-30-13 Fax: + 52 55-56-16-10-73

E-mail: arteaga@verona.fi-p.unam.mx

ABSTRACT

One of the main practical problems on dexterous robots is the complexity of integrating a large amount of sensors within a small robot architecture. In this paper, some experimental results on the control of cooperative robots without using velocity measurements are shown.

Key Words: Experimental results, cooperative robot systems, observer design.

I. INTRODUCTION

Dexterity is one of the most desirable behaviors a robot should be asked to have. This property can be achieved through a robot hand with a combination of good performance between position and force control. Thus, robot hands (as well as cooperative robots), may find many areas of application nowadays [1]. For example, today's industrial robots are characterized by a limited number of specific applications, so that "traditional robotics" requires extending actual industrial robot capabilities. Also, there is a constant interest towards prosthetic devices for humans who have lost their limb. Finally, dexterous tele robotics is an actual desirable technology application.

Early attempts to establish a relationship between the automatic control of robots carrying out a shared task are referred to Kathib's operational space formulation [2]. During the 1980's, the most important research results considered the contact evolution during manipulation [3]. Such a contact evolution requires

a perfect combination of position and force control. Some of the first approaches following the objective of combining position and force control are presented in [4], [5]. In those works, the dynamics of the object is taken into account explicitly. In [6], [7], [8], control schemes which do not take into account the dynamics of the object but rather the motion constraints are designed. These control approaches have the advantage that they do not required an exact knowledge of the system model parameters, since an adaptive approach is introduced. More recently, Shlegl *et al.* shows some advances on hybrid (in terms of a combination of continuous and discrete systems) control approaches [9]. However, despite the fact that Mason proposed the base of sensor-less manipulation in the 1980's [10], there are few control algorithms for cooperative robot systems which take into account the possible lack of velocity measurements. In [11], an observer is introduced. On the other hand, there are relatively few works where the implementation of the different control algorithms is carried out. In this paper we show some experimental outcomes by using the theory presented in [11].

The paper is organized as follows. In Section II, the system model and its properties are presented. Section III recalls the proposed control and observer law given in [11], while Section IV shows the experimental results. Conclusions are drawn in Section V.

II. SYSTEM MODEL AND PROPERTIES

Consider a cooperative system with l -fingers, each of them with n_i degrees of freedom and m_i constraints arising from the contact with an object held by the fingers. Then, the total number of degrees of freedom is given by $n = \sum_1^l n_i$ and $m = \sum_1^l m_i$, $n_i > m_i$. The dynamics of the i -th finger is given by [8]

$$\begin{aligned} \mathbf{H}_i(\mathbf{q}_i)\ddot{\mathbf{q}}_i + \mathbf{C}_i(\mathbf{q}_i, \dot{\mathbf{q}}_i)\dot{\mathbf{q}}_i + \mathbf{D}_i\dot{\mathbf{q}}_i + \mathbf{g}_i(\mathbf{q}_i) &= \boldsymbol{\tau}_i + \mathbf{J}_{\varphi_i}^T(\mathbf{q}_i)\boldsymbol{\lambda}_i, \end{aligned} \quad (1)$$

where $\mathbf{q}_i \in \mathbb{R}^{n_i}$ is the vector of generalized joint coordinates, $\mathbf{H}_i(\mathbf{q}_i) \in \mathbb{R}^{n_i \times n_i}$ is the symmetric positive definite inertia matrix, $\mathbf{C}_i(\mathbf{q}_i, \dot{\mathbf{q}}_i)\dot{\mathbf{q}}_i \in \mathbb{R}^{n_i}$ is the vector of Coriolis and centrifugal torques, $\mathbf{g}_i(\mathbf{q}_i) \in \mathbb{R}^{n_i}$ is the vector of gravitational torques, $\mathbf{D}_i \in \mathbb{R}^{n_i \times n_i}$ is the positive semidefinite diagonal matrix accounting for joint viscous friction coefficients, $\boldsymbol{\tau}_i \in \mathbb{R}^{n_i}$ is the vector of torques acting at the joints, and $\boldsymbol{\lambda}_i \in \mathbb{R}^{m_i}$ is the vector of Lagrange multipliers (physically represents the force applied at the contact point). $\mathbf{J}_{\varphi_i}(\mathbf{q}_i) = \nabla \varphi_i(\mathbf{q}_i) \in \mathbb{R}^{m_i \times n_i}$ is an orthonormal matrix, assumed to be of full rank in this paper. $\nabla \varphi_i(\mathbf{q}_i)$ denotes the gradient of the object surface vector $\varphi_i \in \mathbb{R}^{m_i}$ which maps a vector onto the normal plane at the tangent plane that arises at the contact point described by

$$\varphi_i(\mathbf{q}_i) = \mathbf{0}. \quad (2)$$

Note that equation (2) means that homogeneous constraints are being considered [8]. The complete system is subject to m holonomic constraints given by

$$\varphi(\mathbf{q}) = \mathbf{0}, \quad (3)$$

where $\varphi(\mathbf{q}) = \varphi(\mathbf{q}_1, \dots, \mathbf{q}_l) \in \mathbb{R}^m$. This means that the object being manipulated and the environment are modeled by the constraints (3).

Let us denote the largest (smallest) eigenvalue of a matrix by $\lambda_{\max}(\cdot)$ ($\lambda_{\min}(\cdot)$). The norm of an $n \times 1$ vector \mathbf{x} is defined by $\|\mathbf{x}\| \triangleq \sqrt{\mathbf{x}^T \mathbf{x}}$, while the norm of an $m \times n$ matrix \mathbf{A} is the corresponding induced norm $\|\mathbf{A}\| \triangleq \sqrt{\lambda_{\max}(\mathbf{A}^T \mathbf{A})}$. By recalling that revolute joints are considered, the following property can be established [7], [8]:

Property II.1: The vector $\dot{\mathbf{q}}_i$ can be written as

$$\dot{\mathbf{q}}_i = \dot{\mathbf{q}}_i + (\mathbf{J}_{\varphi_i}^+ \mathbf{J}_{\varphi_i} \dot{\mathbf{q}}_i - \mathbf{J}_{\varphi_i}^+ \mathbf{J}_{\varphi_i} \dot{\mathbf{q}}_i) \quad (4)$$

$$\begin{aligned} &= (\mathbf{I}_{n_i \times n_i} - \mathbf{J}_{\varphi_i}^+ \mathbf{J}_{\varphi_i}) \dot{\mathbf{q}}_i + \mathbf{J}_{\varphi_i}^+ \mathbf{J}_{\varphi_i} \dot{\mathbf{q}}_i \\ &\triangleq \mathbf{Q}_i(\mathbf{q}_i) \dot{\mathbf{q}}_i + \mathbf{J}_{\varphi_i}^+(\mathbf{q}_i) \dot{\mathbf{p}}_i, \end{aligned}$$

where $\mathbf{J}_{\varphi_i}^+ = \mathbf{J}_{\varphi_i}^T (\mathbf{J}_{\varphi_i} \mathbf{J}_{\varphi_i}^T)^{-1} \in \mathbb{R}^{n_i \times m_i}$ stands for the Penrose's pseudo inverse and $\mathbf{Q}_i \in \mathbb{R}^{n_i \times n_i}$ satisfies $\text{rank}(\mathbf{Q}_i) = n_i - m_i$. These two matrices are orthogonal, i.e. $\mathbf{Q}_i \mathbf{J}_{\varphi_i}^+ = \mathbf{O}$ (and $\mathbf{Q}_i \mathbf{J}_{\varphi_i}^T = \mathbf{O}$). $\dot{\mathbf{p}}_i = \mathbf{J}_{\varphi_i} \dot{\mathbf{q}}_i \in \mathbb{R}^{m_i}$ is the so called constrained velocity. Furthermore, in view of constraint (3), it holds

$$\sum_{i=1}^l \dot{\mathbf{p}}_i = \mathbf{0} \quad \text{and} \quad \sum_{i=1}^l \mathbf{p}_i = \sum_{i=1}^l \int_0^t \mathbf{J}_{\varphi_i} \dot{\mathbf{q}}_i dt = \mathbf{0}. \quad (5)$$

Since homogeneous constraints are being considered, it also holds in view of (2) that

$$\dot{\mathbf{p}}_i = \mathbf{0} \quad \text{and} \quad \mathbf{p}_i = \mathbf{0}, \quad (6)$$

for $i = 1, \dots, l$. \mathbf{p}_i is called the constrained position.

\triangleq

III. CONTROL WITH VELOCITY ESTIMATION

In this section, the control and observer scheme for cooperative systems presented in [11] are written down. Consider model (1) and define the tracking and observation errors as $\tilde{\mathbf{q}}_i \triangleq \mathbf{q}_i - \mathbf{q}_{di}$, $\mathbf{z}_i \triangleq \mathbf{q}_i - \hat{\mathbf{q}}_i$, where \mathbf{q}_{di} is a desired smooth bounded trajectory satisfying constraint (2), and (\cdot) represents the estimated value of (\cdot) . Other error definitions are $\Delta \mathbf{p}_i \triangleq \mathbf{p}_i - \mathbf{p}_{di}$, $\Delta \boldsymbol{\lambda}_i \triangleq \boldsymbol{\lambda}_i - \boldsymbol{\lambda}_{di}$, where \mathbf{p}_{di} is the desired constrained position which satisfies (6). $\boldsymbol{\lambda}_{di}$ is the desired force to be applied by each finger on the constrained surface. Other useful definitions are

$$\dot{\mathbf{q}}_{ri} \triangleq \mathbf{Q}_i(\mathbf{q}_i) (\dot{\mathbf{q}}_{di} - \boldsymbol{\Lambda}_i (\hat{\mathbf{q}}_i - \mathbf{q}_{di})) \quad (7)$$

$$+ \mathbf{J}_{\varphi_i}^+(\mathbf{q}_i) (\dot{\mathbf{p}}_{di} - \beta_i \Delta \mathbf{p}_i + \boldsymbol{\xi}_i \Delta \mathbf{F}_i)$$

$$\mathbf{s}_i \triangleq \dot{\mathbf{q}}_i - \dot{\mathbf{q}}_{ri} \quad (8)$$

$$= \mathbf{Q}_i(\mathbf{q}_i) (\dot{\tilde{\mathbf{q}}}_i + \boldsymbol{\Lambda}_i (\hat{\mathbf{q}}_i - \mathbf{q}_{di}))$$

$$+ \mathbf{J}_{\varphi_i}^+(\mathbf{q}_i) (\Delta \dot{\mathbf{p}}_i + \beta_i \Delta \mathbf{p}_i - \boldsymbol{\xi}_i \Delta \mathbf{F}_i) \quad (9)$$

$$\Delta \mathbf{F}_i \triangleq \int_0^t \Delta \boldsymbol{\lambda}_i(\vartheta) d\vartheta \quad (10)$$

where $\boldsymbol{\Lambda}_i \in \mathbb{R}^{n_i \times n_i}$, $\boldsymbol{\xi}_i \in \mathbb{R}^{m_i \times m_i}$ are diagonal positive definite matrices, and β_i is a positive constant. Let us define

$$\begin{aligned} \ddot{\mathbf{q}}_{ri} &\triangleq \dot{\mathbf{Q}}_i(\mathbf{q}_i) (\dot{\mathbf{q}}_{di} - \boldsymbol{\Lambda}_i (\hat{\mathbf{q}}_i - \mathbf{q}_{di})) \\ &+ \dot{\mathbf{J}}_{\varphi_i}^+(\mathbf{q}_i) (\dot{\mathbf{p}}_{di} - \beta_i \Delta \mathbf{p}_i + \boldsymbol{\xi}_i \Delta \mathbf{F}_i) \end{aligned} \quad (11)$$

$$\begin{aligned}
& + \mathbf{Q}_i(\mathbf{q}_i) \left(\ddot{\mathbf{q}}_{di} - \boldsymbol{\Lambda}_i \left(\dot{\mathbf{q}}_i - \dot{\mathbf{q}}_{di} \right) \right) \\
& + \mathbf{J}_{\varphi_i}^+(\mathbf{q}_i) (\ddot{\mathbf{p}}_{di} - \beta_i (\mathbf{J}_{\varphi_i}(\mathbf{q}_i) \dot{\mathbf{q}}_{oi} - \dot{\mathbf{p}}_{di}) + \boldsymbol{\xi}_i \Delta \boldsymbol{\lambda}_i),
\end{aligned}$$

where $\dot{\mathbf{Q}}_i(\mathbf{q}_i)$ and $\dot{\mathbf{J}}_{\varphi_i}^+(\mathbf{q}_i)$ are given in [11]. The proposed controller is then given for each single robot by

$$\begin{aligned}
\boldsymbol{\tau}_i & \triangleq \mathbf{H}_i(\mathbf{q}_i) \ddot{\mathbf{q}}_{ri} + \mathbf{C}_i(\mathbf{q}_i, \dot{\mathbf{q}}_{ri}) \dot{\mathbf{q}}_{ri} \\
& + \mathbf{D}_i \dot{\mathbf{q}}_{ri} + \mathbf{g}_i(\mathbf{q}_i) \\
& - \mathbf{K}_{R_i} (\dot{\mathbf{q}}_{oi} - \dot{\mathbf{q}}_{ri}) - \mathbf{J}_{\varphi_i}^T(\mathbf{q}_i) (\boldsymbol{\lambda}_{di} - k_{F_i} \Delta \mathbf{F}_i),
\end{aligned} \tag{12}$$

where $\mathbf{K}_{R_i} \in \mathbb{R}^{n_i \times n_i}$ is a diagonal positive definite matrix and k_{F_i} is a positive constant.

The proposed dynamics of the observer is given by

$$\dot{\mathbf{q}}_i = \dot{\mathbf{q}}_{oi} + \boldsymbol{\Lambda}_i \mathbf{z}_i + k_{di} \mathbf{z}_i \tag{13}$$

$$\begin{aligned}
\ddot{\mathbf{q}}_{oi} & = \ddot{\mathbf{q}}_{ri} + k_{di} \boldsymbol{\Lambda}_i \mathbf{z}_i \\
& + \mathbf{H}_i^{-1}(\mathbf{q}_i) \mathbf{J}_{\varphi_i}^T(\mathbf{q}_i) (\Delta \boldsymbol{\lambda}_i + k_{F_i} \Delta \mathbf{F}_i),
\end{aligned} \tag{14}$$

where k_{di} is a positive constant. Then, gains can be found such that

$$\lim_{t \rightarrow \infty} \dot{\mathbf{q}}_i = \mathbf{0} \quad \lim_{t \rightarrow \infty} \ddot{\mathbf{q}}_i = \mathbf{0} \quad \lim_{t \rightarrow \infty} \dot{\mathbf{z}}_i = \mathbf{0} \tag{15}$$

$$\lim_{t \rightarrow \infty} \mathbf{z}_i = \mathbf{0} \quad \lim_{t \rightarrow \infty} \Delta \boldsymbol{\lambda}_i = \mathbf{0}. \tag{16}$$

The proof of this statement, together with the conditions necessary to guarantee stability, can be found in [11].

IV. EXPERIMENTAL RESULTS

In this section, the experimental results are presented. To this end, a test bed with two industrial robots is used (Figure 1). The robots are at the Laboratory for Robotics of the National University of Mexico. They are the A465 and A255 of *CRS Robotics*. Even though the first one has six degrees of freedom and the second one five, only the first three joints of each robot are used for the experiments, while the rest of them are mechanically braked. Each joint is actuated by a CD motor. Thus, in order to implement control law (12) and observer (13)–(14), the motors dynamics has to be taken into account. Furthermore, as it may be appreciated in Figure 1, only the robot A465 has a force sensor. For this reason, the trajectories to be followed must be relative simple, so that the single measurements of the single force sensor can be used for the two manipulators.

The palm frame of the whole system is at the base of the robot A465, with its x -axis pointing towards

the other manipulator. If the task consists in lifting the object and pushing with a desired force, then the constraints in Cartesian coordinates are simply given by

$$\varphi_i = x_i - b_i = 0, \tag{17}$$

for $i = 1, 2$ and b_i a positive constant. The desired trajectories are given

$$x_{d1} = 0.626[\text{m}] \quad x_{d2} = 0.936[\text{m}] \tag{18}$$

$$y_{d1,2} = 0.05 \sin(\omega(t - t_i))[\text{m}] \tag{19}$$

$$z_{d1,2} = (0.585 + 0.05 \cos(\omega(t - t_i)) - 0.05)[\text{m}] \tag{20}$$

Note that the inverse kinematics of the manipulators has to be employed to compute \mathbf{q}_{di} , for $i = 1, 2$. These trajectories are valid from an initial time t_i to a final time t_f , while ω is a fifth order polynomial designed to satisfy $\omega(t_i) = \omega(t_f) = 0$. Also, the derivatives of ω are zero at t_i and t_f . By choosing (18)–(19), the robots will make a circle in the y - z plane. Note that the only difference between the trajectories for robots A465 and A255 is the width of the object. Also, no force control is carried until the manipulators are in the initial position for the circle, at $(0.626, 0, 0.585)[\text{m}]$ for the first robot and $(0.936, 0, 0.585)[\text{m}]$ for the second one. The desired pushing force is chosen as

$$f_{dx1,2} = 15 + 5 \sin(2\pi(t - t_i)/40)[\text{N}], \tag{21}$$

and $f_{dy1,2} = f_{dz1,2} = 0[\text{N}]$. Note that in view of the desired trajectories, the force read by the single sensor can be used for both robots. The different control and observer parameters are $\boldsymbol{\Lambda}_1 = 12\mathbf{I}$, $\boldsymbol{\Lambda}_2 = 23\mathbf{I}$, $\mathbf{K}_{R_1} = \text{diag}\{45 \ 60 \ 60\}$, $\mathbf{K}_{R_2} = \text{diag}\{15 \ 13 \ 13\}$, $k_{d1} = k_{d2} = 4$, $k_{f1} = k_{f2} = 5$, $\boldsymbol{\xi}_1 = \boldsymbol{\xi}_2 = 0.001\mathbf{I}$.

The observer-controller scheme has been programmed in a PC computer, with a sampling time of 9ms. The results for the desired force (21) for the tracking errors can be seen in Figure 2 in joint coordinates, and in Figure 3 in Cartesian coordinates. Only the time from $t_i = 15\text{s}$ to $t_f = 55\text{s}$ is shown because otherwise no force control is being used. It can be appreciated that the errors are relatively large. This is mainly to the fact that an exact knowledge of the manipulators dynamics is required, while the models used in the experiments are not very accurate. On

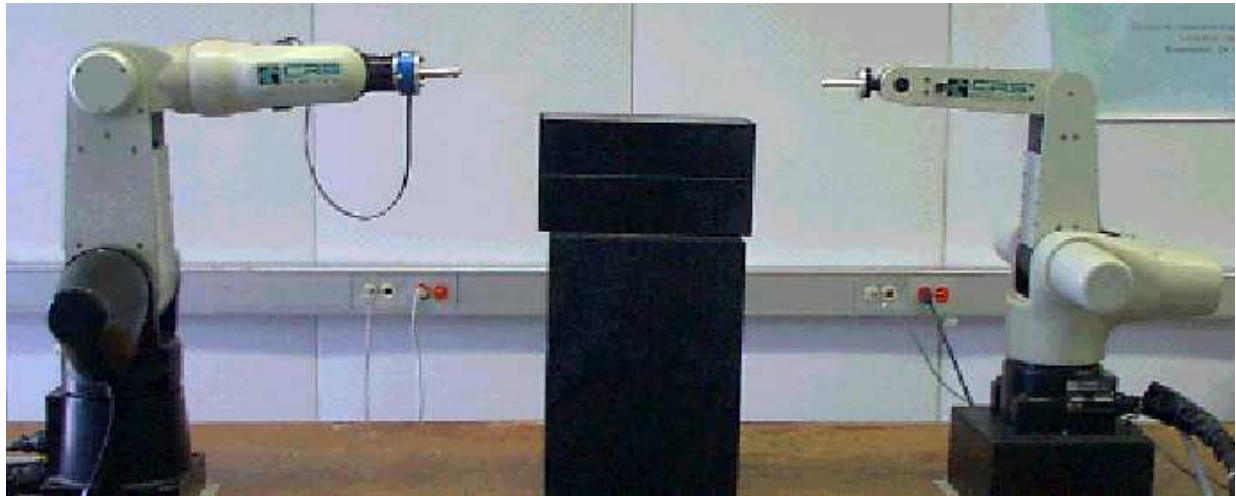


Fig. 1: Robots A465 and A255 of CRS Robotics.

the other hand, for the desired force (21) the results can be considered pretty good, although one can only show the real force for the robot A465 (Figure 4). This demonstrates the efficacy of designing a decentralized controller. Figure 5 shows the observation errors. As can be appreciated, they are pretty good as well. Since the observer uses little information from the robots dynamics, this rather confirms that the tracking errors could be improved by taking into account more accurate models of the manipulators.

V. CONCLUSIONS

By using a known control law for tracking control of cooperative robots without velocity measurements, experimental results are considered in this paper. The test bed is made up of two industrial robots. A desired time varying force signal is chosen, while the spatial trajectory is a circle. Since only one robot owns a force sensor, the outcomes were better for this one than for other. However, the overall results can be considered good, even though it has become clear that the approach should be modified to take into account inaccuracies in the robot model and the possible lack of force sensors.

Acknowledgments

This work is based on research supported by the DGAPA-UNAM under grant **IN106901**.

REFERENCES

- [1] R. M. Murray, Z. Li, and S. S. Sastry, *A Mathematical Introduction to Robotic Manipulation*, CRC Press, Boca Raton, Florida, U. S. A., 1994.
- [2] O. Khatib, "A unified approach for motion and force control of robot manipulators: The operational space formulation", *IEEE Journal on Robotics and Automation*, vol. 3, pp. 43–53, 1987.
- [3] D. J. Montana, "The kinematics of contact and grasp", *International Journal of Robotics Research*, vol. 7, no. 3, 1988.
- [4] Z. Li, P. Hsu, and S. Sastry, "Grasping and coordinated manipulation by a multifingered robot hand", *International Journal of Robotics Research*, vol. 8, no. 4, pp. 33–50, 1989.
- [5] A. Cole, "Constrained motion of grasped objects by hybrid control", in *Proceedings of the 1990 IEEE International Conference on Robotics and Automation*, 1990, pp. 1954–1960.
- [6] V. Parra-Vega and S. Arimoto, "A passivity-based adaptive sliding mode position-force control for robot manipulators", *International Journal of Adaptive Control and Signal Processing*, vol. 10, pp. 365–377, 1996.
- [7] Y.-H. Liu, S. Arimoto, V. Parra-Vega, and K. Kitagaki, "Decentralized adaptive control of multiple manipulators in cooperations", *International Journal of Control*, vol. 67, no. 5, pp. 649–673, 1997.
- [8] V. Parra-Vega, A. Rodríguez-Ángeles, S. Arimoto, and G. Hirzinger, "High precision constrained grasping with cooperative adaptive handcontrol", *Journal of Intelligent and Robotic Systems*, vol. 32, pp. 235–254, 2001.
- [9] T. Schlegel, M. Buss, T. Omata, and G. Schmidt, "Fast dextrous regrasping with optimal contact forces and contact sensor based impedance control", in *Proc. IEEE Int. Conf. on Robotics and Automation*, 2001, pp. 103–109.
- [10] M. T. Mason and J. K. Salisbury, *Robot Hands and the Mechanics of Manipulation*, The MIT Press, London, 1985.
- [11] A. Arteaga Pérez, M. A. y Muñoz, "Control of cooperative robots without velocity measurements", in *Proc. CD ROM, IROS 2002 IEEE/RSJ International Conference on Intelligent Robots and Systems*, Lausanne, Switzerland, September–October 2002, pp. 2837–2842.

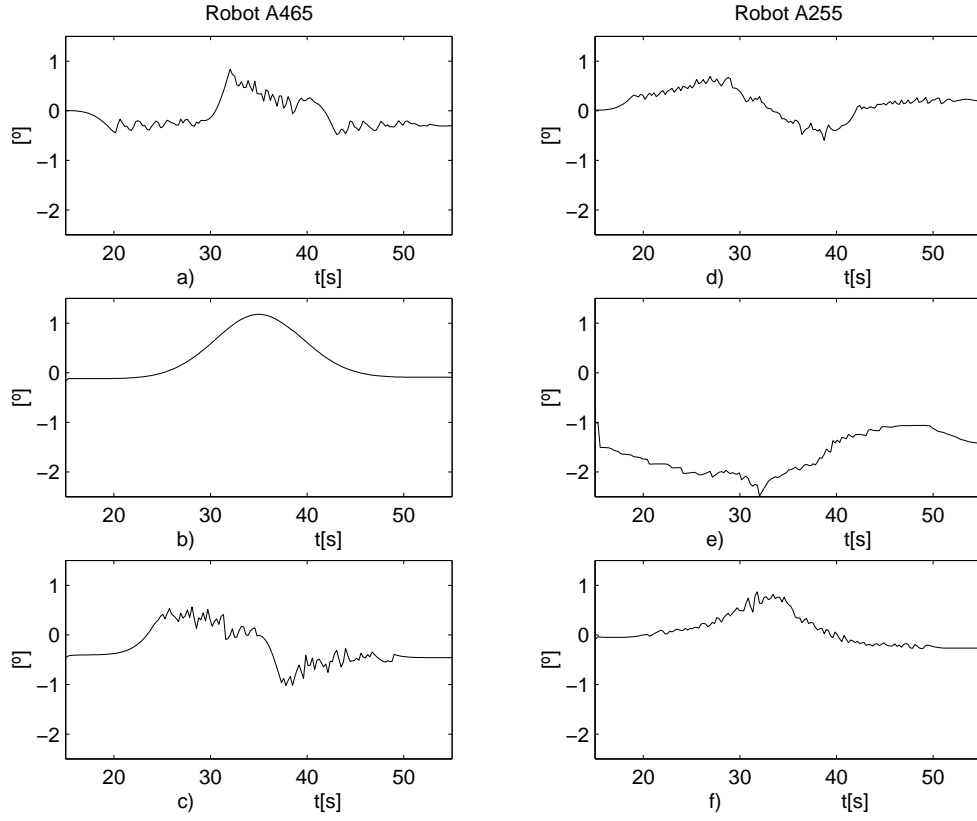


Fig. 2: Tracking errors in joint coordinates for (21). a) \tilde{q}_{11} . b) \tilde{q}_{12} . c) \tilde{q}_{13} . d) \tilde{q}_{21} . e) \tilde{q}_{22} . f) \tilde{q}_{23} .

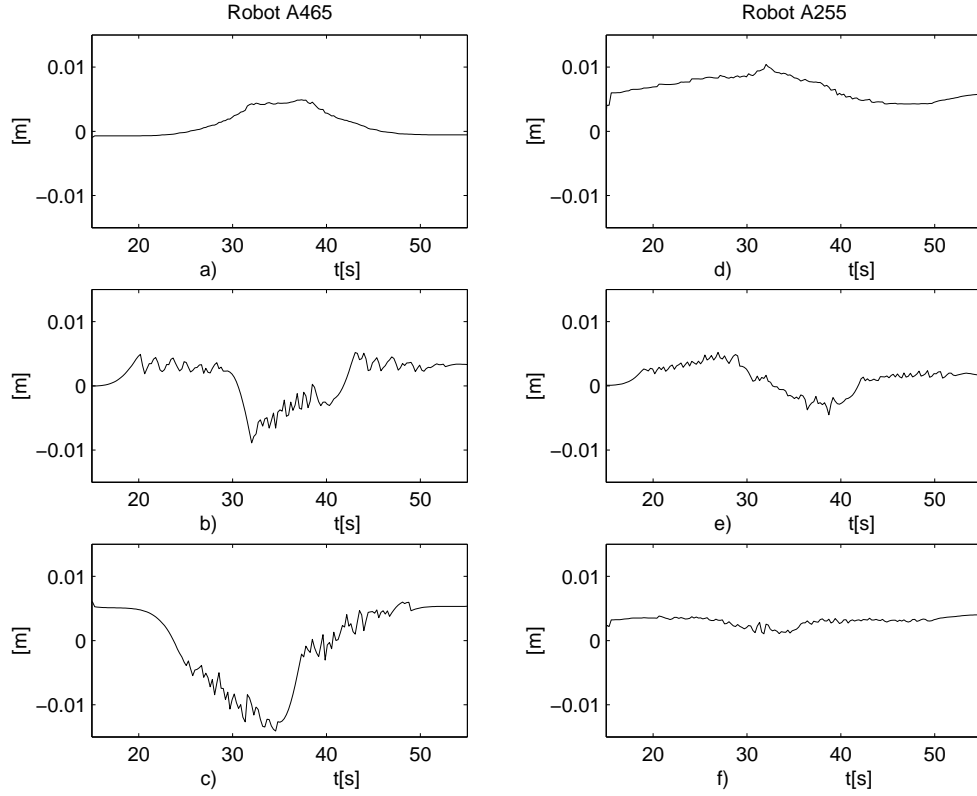


Fig. 3: Tracking errors in Cartesian coordinates for (21). a) \tilde{x}_1 . b) \tilde{y}_1 . c) \tilde{z}_1 . d) \tilde{x}_2 . e) \tilde{y}_2 . f) \tilde{z}_2 .

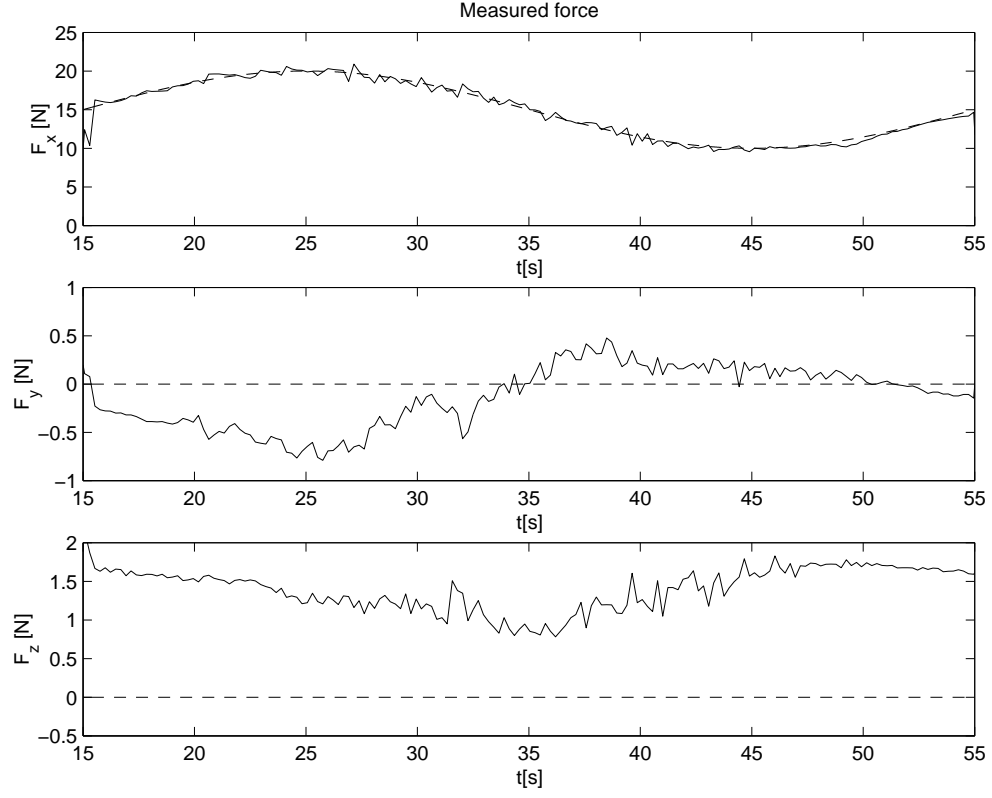


Fig. 4: Force measurements for (21). a) F_{x_1} . b) F_{y_1} . c) F_{z_1} . — measured value. - - - desired value.

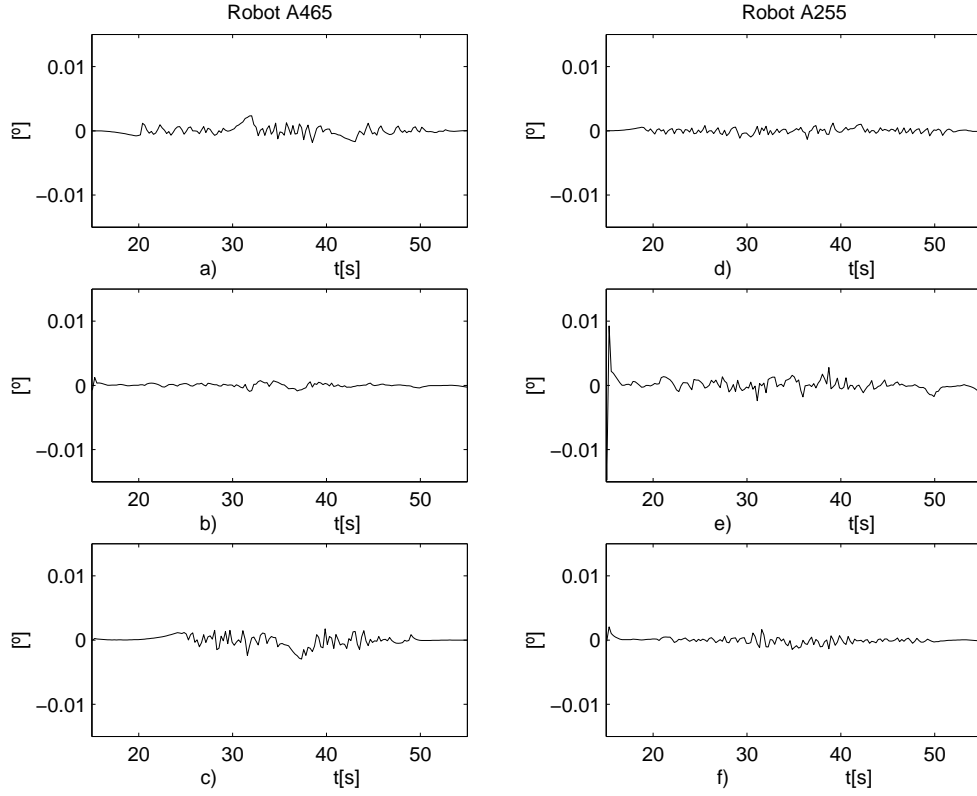


Fig. 5: Observation errors for (21). a) z_{11} . b) z_{12} . c) z_{13} . d) z_{21} . e) z_{22} . f) z_{23} .